Electrochemical characterization of the solvent-enhanced conductivity of poly(3,4-ethylenedioxythiophene) and its application in polymer solar cells†

Jen-Hsien Huang,[a] Dhananjay Kekuda,[c] Chih-Wei Chu*[cd] and Kuo-Chuan Ho*[ab]

Received 17th December 2008, Accepted 13th March 2009
First published as an Advance Article on the web 20th April 2009
DOI: 10.1039/b822729b

The influence of solvent on the electrochemical property and conductivity of PEDOT has been investigated by electrochemical and physical characterizations. The PEDOT treated with different solvents reveals a different reversibility of ionic transport and cycling stability, which is associated with the conformational rearrangement from aggregated to linear polymer chains, as evidenced from atomic force microscopy (AFM). The conductivity of the PEDOT thin film can also be enhanced while the degree of linear polymer chains is higher. The application of highly conductive PEDOT thin film as a buffer layer in the polymer photovoltaic devices was realized. A PCE of 4.27% for photovoltaic devices based on P3HT–PCBM under simulated sun light is achieved by using a PEDOT thin film treated with DMSO.

1 Introduction

Poly(3,4-ethylenedioxythiophene) (PEDOT) doped with poly-(styrene sulfonate) (PSS) is among the most successful conjugated polymers in commercial applications since it was synthesized in the late 1980s. Recently, solution processable PEDOT–PSS have been paid much attention as active materials in electrochromic devices, as thin buffer layers in organic electronics, or as conductive electrodes due to their remarkable chemical inertness, high thermal stability, tunable optical and electrical properties. Although the flexible PEDOT–PSS films have been applied extensively in many optoelectronic devices, the major challenge of the solution processable PEDOT–PSS is their low conductivity compared with the inorganic conductors such as indium tin oxide (ITO), resulting in reduction of the performance of the opto-electronic devices. In light of these issues, it is necessary to develop polymer films with high conductivity without losing its transparency to satisfy the demand for the optoelectronic applications.

It has been discovered that the conductivity of the PEDOT–PSS films could be enhanced more than an order of magnitude by the addition of polyalcohols such as sorbitol, glycerol and ethylene glycol (EG) or high-dielectric solvents such as dimethyl sulfoxide (DMSO), *N*,*N*-dimethylformamide (DMF) and utilized them as buffer layer in polymer solar cells.[1,2] Several groups have studied the fundamental causes for the conductivity enhancement of PEDOT–PSS and proposed the suitable mechanisms. Inganäs *et al.* consider the high boiling points of sorbitol or glycerol that act as a plasticizer, which increases the re-orientation of the PEDOT–PSS chains under annealing leading to a better intra-chains reaction.[3,4] Ashizawa *et al.* suggested the mixed solution of PEDOT–PSS and EG can form a gel leading to a three dimension network of the PEDOT–PSS, which can enhance the hopping of charge carriers.[5] Timpanaro *et al.* proposed the addition of sorbitol resulting in clustering of PEDOT–PSS into bigger aggregates, which enhanced the formation of conductive pathway.[6] Friend *et al.* observed the improved conductivity in the presence of glycerol is due to swelling and aggregation of the colloidal PEDOT particles forming a highly conductive network.[7] Kim *et al.* considered the polar solvents with high dielectric constants, which induced strong screening effects.[8] This reduces the Coulombic interactions between the counter ions and the charge carrier leading to a higher conductivity. Jönsson *et al.* suggested that the insulating PSS segments can be removed from the PEDOT–PSS surface with the addition of the sorbitol during film formation and produced better connection between the conducting PEDOT.[9] Crispin *et al.* proposed that EG can reduce the PEDOT–PSS grain size leading to a thinner PSS layer around the conductive PEDOT particles.[10] Ouyang *et al.* concluded that the conformation of PEDOT film undergoes a rearrangement from aggregated to linear or expanded-aggregated polymer chains with the addition of DMSO or EG.[11] They proposed that the conformational change of PEDOT chains is contributed from the interaction between the dipole of organic solvent and the dipoles on the PEDOT chains. Bagchi *et al.* also estimated the radius of gyration from small-angle X-ray scattering (SAXS) to identify the Guinier regime.[12] Although extensive works have been completed to date, the mechanism for this observation has been debated and a conclusive explanation for the conductivity increase is still lacking so far.

In this study, we employed the highly conductive PEDOT films as the hole collection layer in bulk heterojunction solar cell based on poly(3-hexylthiophene) (P3HT) and [6,6]-phenyl C_{61}-butyric acid methyl ester (PCBM). In order to investigate the conductivity enhancement of PEDOT dominated by the PSS or solvents,

[a]*Department of Chemical Engineering, National Taiwan University, Taipei, Taiwan. E-mail: kcho@ntu.edu.tw; Fax: +886-2-23623040; Tel: +886-2-23660739*
[b]*Institute of Polymer Science and Engineering, National Taiwan University, Taipei, Taiwan*
[c]*Research Center for Applied Sciences, Academia Sinica, Taipei, Taiwan. E-mail: gchu@gate.sinica.edu.tw; Fax: +886-2-27826680; Tel: +886-2-27898000 ext. 70*
[d]*Department of Photonics National Chiao Tung University, Hsinchu, Taiwan*

† Electronic supplementary information (ESI) available: Detailed results of x_R and x_O. See DOI: 10.1039/b822729b

the PEDOT films were prepared *via* oxidative polymerization with iron(III) *p*-toluenesulfonate ($Fe(OTs)_3$) as the oxidative agent to exclude the effect of PSS polymer segments. Furthermore, we employed cyclic voltammetry (CV) and an electrochemical quartz crystal microbalance (EQCM) to investigate the influence of the polymer conformation which is treated by solvents. The ions, which participate in the redox process and the contribution of cations and anions to charge-compensation motion during the injection/ejection of electrons in PEDOT films, can lead to a mass change. Therefore we can use the mass changes under different solvents to propose a reasonable mechanism of conductivity enhancement of PEDOT films.

2. Experimental

The PEDOT films were synthesized *via* oxidative polymerization. The oxidative polymerization was carried out according to the procedure reported in literature.[13,14] Firstly, the oxidant (iron(III) *p*-toluenesulfonate ($Fe(OTs)_3$)) and weak base (imidazole (Im)) were dissolved separately in a methanol solution. Then, the monomer was mixed with Im and $Fe(OTs)_3$ solutions and the molar ratio of $Fe(OTs)_3$–monomer was controlled at 1.75 : 1. The mixture was spin-coated onto ITO substrates (sheet resistance = 20 Ω per sq., RiTdisplay Corporation, Hsinchu Industrial Park, Taiwan) and heated at 100 °C subsequently. Finally, the PEDOT film was rinsed by methanol several times to remove the oxidative agent and Im and dried in N_2 atmosphere. Subsequently, the PEDOT was treated with four different solvents before characterization. The films were cycled in acetonitrile (ACN), DMF, EG and DMSO between −0.3 and 0.9 V (*vs.* Ag/Ag^+(containing 0.01 M $AgNO_3$ and 0.1 M $TBAClO_4$ in ACN)) and then soaked in these solvents for 72 h at RT. Then, the samples were dried in a vacuum oven at 60 °C for 12 h. CV studies were performed with a three-electrode cell with 0.1 M $LiClO_4$/ACN using ITO as the working electrode, a platinum sheet as the counter electrode, and non-aqueous Ag/Ag^+ as the reference electrode. Spectroelectrochemical data were recorded on a Shimadzu model UV-1601PC spectrophotometer. EQCM investigations were carried using a quartz crystal analyzer (Seiko EG&G, QCA917) connected to an Autolab potentiostat/galvanostat. The mass changes per active area were calculated by the Sauerbrey equation:[15]

$$\Delta m = \frac{(N \times r_q)}{f_0^2} \times \Delta f \quad (1)$$

where N is the shear modulus of quartz (167 kHz cm), r_q is the density of the crystal (2.684 g cm^{-3}), f_0 is the resonant frequency of the fundamental mode of the crystal (8.88 MHz), and Δf is the resonance frequency shift during redox cycling. The sensitivity of the EQCM apparatus used was 5.608 ng Hz^{-1}. The conductivity of PEDOT films were measured by a four-point probe. Surface morphorlogy of polymer films were obtained using atomic force microscopy (AFM, Digital instrument NS 3a controller with D3100 stage).

The polymer photovoltaic devices were fabricated by spin-coating blend of P3HT:PCBM on the PEDOT modified ITO surface. Prior to the deposition, the blend of P3HT:PCBM was prepared by dissolving it in 1,2-dichlorobenzene with 1 : 0.8 weight ratio, followed by stirring the solution for 12 h at 50 °C. The active layer was obtained by spin-coating the blend at 600 rpm for 60 s. The active layer was then dried in covered Petri glass dishes. Subsequently, the films were annealed on the top of hotplate at 130 °C. A 30 and 100 nm thick of calcium and aluminum, respectively, was thermally evaporated under vacuum at a pressure below 6×10^{-6} Torr through a shadow mask. The active area of the device was controlled at 0.1 cm^2. The hole only devices were fabricated by replacing Ca with higher work function MoO_3 (Φ = 5.3 eV) as the top electrode.[16] The MoO_3 was thermally evaporated with a thickness of 20 nm and then capped with 50 nm of Al. For the electron only devices, PEDOT–PSS layer was replaced with $CsCO_3$ (Φ = 2.9 eV), which was thermally evaporated with a thickness of 2 nm.[17] The active layers were annealed at 130 °C for 20 min before the hole and electron only devices were fabricated. The solar cell testing was done inside a glove box under simulated AM 1.5G irradiation (100 W cm^{-2}) using a xenon lamp based solar simulator (Thermal Oriel 1000 W). The light intensity was calibrated by a mono-silicon photodiode with KG-5 colour filter (Hamamatsu, Inc.). The whole measurement was performed in a glove box filled with N_2 at room temperature.

3. Results and discussion

3.1 The investigation on the mechanism of conductivity enhancement in PEDOT

Fig. 1 shows the mass and current response during the CV scan stepped between −0.9 and 0.3 V. It can be seen the mass change of PEDOT films do not return to their initial values. The mass of PEDOT film increased about 4500 ng in 0.1 M $LiClO_4$–ACN after 100 cycles. Although the same tendency of mass change in DMF is observed (Fig. 1 (b)), the accumulated mass in DMF is much smaller (800 *vs.* 4500 ng) after 100 cycles compared with the case in ACN, which means that the ion exchange is more reversible in DMF. In the cases of EG and DMSO, the mass just increase 440 and 290 ng even after 100 cycles, respectively (Fig. 1 (c) and (d)). The irreversibility of PEDOT in the various electrolytes is due to the fact that cations or anions can be easily transferred into polymer but cannot be ejected during redox, which was also observed by Plieth and co-workers.[18] The enhancement of reversibility in terms of ionic transfer is resulted from the conformational transition of PEDOT from aggregated to linear structure. The linear structure promotes the reversibility of ionic transfer leading to a smaller accumulated mass.

Fig. 2 shows the charge capacity variations compared with the 1st cycle of PEDOT electrode as a function of cycle number while performing CV from the 1st to the 100th cycle (at a scan rate of 100 mV s^{-1}) in different electrolytes. The potential range of CV was between 0.3 and −0.9 V. It can be seen that PEDOT shows a continuous decay in the charge capacity in these electrolytes. The continuous decay in charge capacity is due to the irreversibility of ion transfer. The charge compensation of PEDOT is accomplished by cations and anions during redox process. A portion of ion pairs transported into the polymer film without ejection was found in the four electrolytes as shown in Fig. 1. Once the ion pairs were trapped into polymer chains, the trapped site can not receive other ions to achieve electroneutralization and the polymer would lose the electroactivity gradually. For $LiClO_4$–DMSO electrolyte, however, the charge

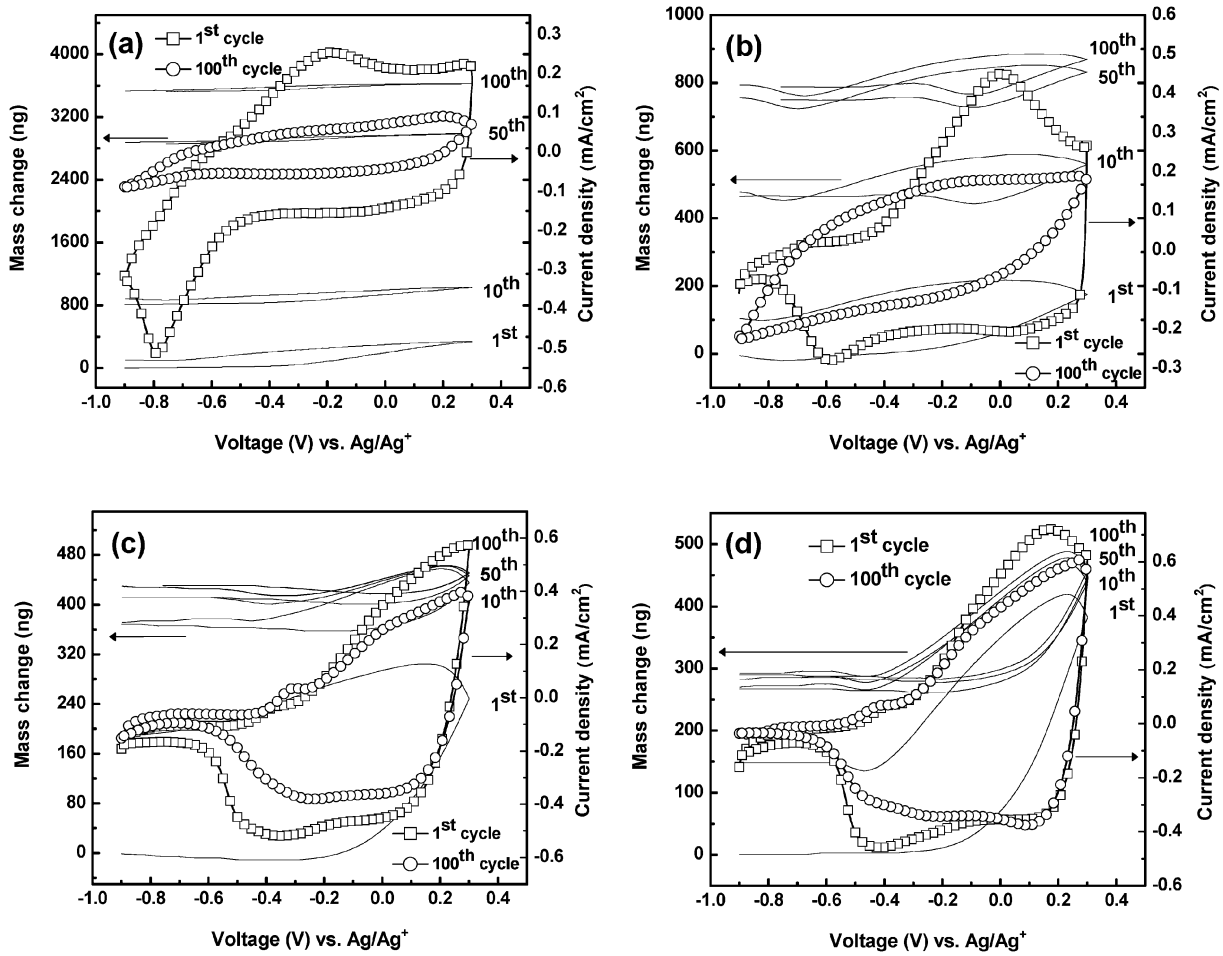

Fig. 1 Δm–E plots for PEDOT cycled between −0.9 and 0.3 V (*vs.* $Ag/Ag^+(AN)$) in (a) ACN, (b) DMF, (c) EG and (d) DMSO with 0.1 M $LiClO_4$. Scan rate: 50 mV s^{-1}.

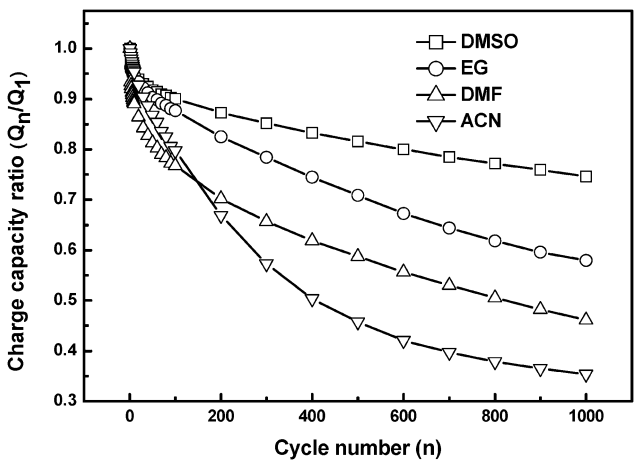

Fig. 2 Variation of the charge capacities of PEDOT films as a function of cycle number in different electrolytes. The CV was scanned from 0.3 to −0.9 V at a scan rate of 50 mV s^{-1}.

capacity ratio is the highest compared with other mediums. After 1000 cycles, the capacity ratio of PEDOT in 0.1 M $LiClO_4$–DMSO can still maintain 75%, which is quite larger than the one in ACN (35%).

Table 1 The conductivity of PEDOT films treated from various solvents

Sample	Conductivity/S cm^{-1}
PEDOT (pristine)	150 ± 0.1
PEDOT treated from ACN	155 ± 0.5
PEDOT treated from DMF	243 ± 1.0
PEDOT treated from EG	311 ± 5.0
PEDOT treated from DMSO	347 ± 5.0

Table 1 shows the conductivity of PEDOT films treated with various solvents. The conductivities of pristine PEDOT film and the one treated from ACN, DMF, EG and DMSO are ~150, ~155, ~243, ~311 and ~347 S cm^{-1}, respectively. The interaction between the dipole of the organic molecular (DMSO or EG) and the dipoles or charges on the PEDOT chains leads to a conformational changes from aggregated to linear structure. The PEDOT chains with linear structure can promote the charge hopping leading to a higher conductivity.[19] In order to develop inexpensive renewable energy sources, extensive works in different device configurations have been accomplished to fabricate ITO free photovoltaic devices.[20–25] With the high conductivity of PEDOT, it is possible to use the

highly conductive PEDOT treated with DMSO or EG to replace of the expensive and hard ITO substrate to fabricate the ITO free organic solar cells. This is quite crucial for development of low-cost, lightweight, efficient and flexible photovoltaic devices.

In order to investigate how the electrolytes influence the ionic reversibility of PEDOT, the behaviour of ionic transport is explored and the global mass and charge balance are used as following equations:

$$\Delta m_{(E)} = W_C n_{C(E)} + W_A n_{A(E)} + W_S n_{S(E)} \quad (2)$$

$$\Delta Q_{(E)} = z_A F n_{A(E)} - z_C F n_{C(E)} \quad (3)$$

where W_i is molar mass of cations (C), anions (A), or solvent molecules (S), $z_i F$ is the absolute value of the electronic charge on each mole of species i, and $n_{i(E)}$ represents the amount of exchanged species i at a specific potential. It has been shown that both anions and cations are involved in *n*-doping as well as in *p*-doping processes for PEDOT and other conducting polymers.[26–28] Furthermore, the continuous decay in charge capacity is resulted from the trapping of cations and anions as shown in Fig. 1, therefore we eliminate the term of solvent to simplify the equation. Subsequently, an expression to calculate the instantaneous molar flux in the redox process within the film as a function of potential was obtained by combining eqn (2) and eqn (3) and considering z_A and $z_C = 1$.[29,30]

$$\frac{1}{A}\frac{dn_{C(E)}}{dt} = \frac{1}{A(W_C+W_A)}\frac{d(\Delta m_{(E)})}{dt} - \frac{W_A}{A(W_C+W_A)}\left(\frac{1}{F}\frac{dQ_{(E)}}{dt}\right) \quad (4)$$

$$\frac{1}{A}\frac{dn_{A(E)}}{dt} = \frac{1}{A(W_C+W_A)}\frac{d(\Delta m_{(E)})}{dt} + \frac{W_C}{A(W_C+W_A)}\left(\frac{1}{F}\frac{dQ_{(E)}}{dt}\right) \quad (5)$$

where A is the piezoelectrically active surface area. When a species is inserted, the flux is considered positive, and they are extracted in the negative case. Fig. 3 illustrates the plots of these differential quantities (cations, anions, and electrons) as a function of the potential for PEDOT scanned in different solvents for the 20th cycle. During the reduction scan, Li^+ and ClO_4^- were inserted into and ejected out of the PEDOT thin film, respectively, as shown in Fig. 3. Fig. 3 also exhibits that the absolute values of the molar fluxes of Li^+ were larger than those of ClO_4^- during the entire redox reaction. The ionic radii of Li^+ and ClO_4^- are 76 and 237 pm, respectively.[31] This means the larger flux of Li^+ can be explained by the smaller ionic size, which allows a better migration. The observation infers that the

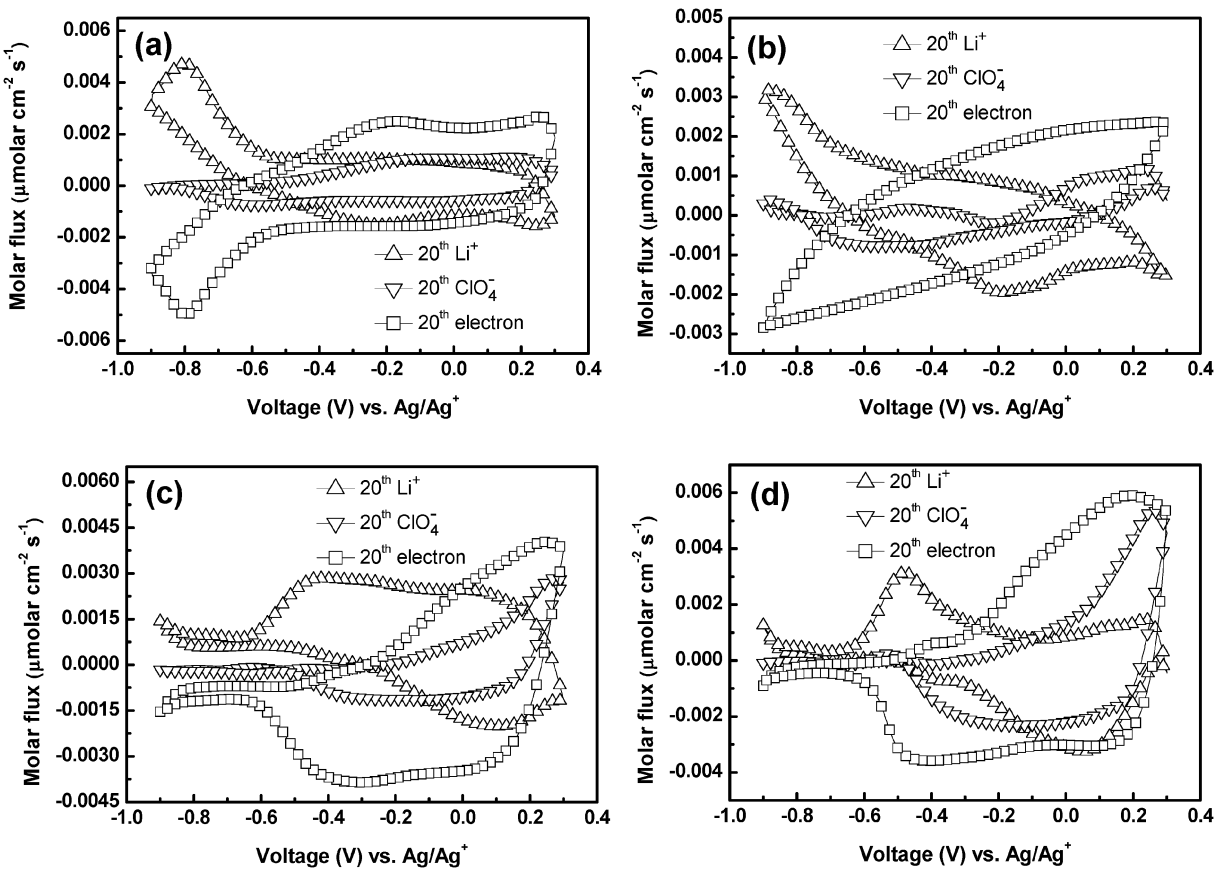

Fig. 3 Calculated molar fluxes of Li^+, ClO_4^-, and electrons for PEDOT films cycled between 0.3 and −0.9 V (*vs.* Ag/Ag^+(AN)) for the 20th cycle in (a) 0.1 M $LiClO_4$–ACN, (b) 0.1 M $LiClO_4$–DMF, (c) 0.1 M $LiClO_4$–EG, (d) 0.1 M $LiClO_4$–DMSO. The scan rate was 50 mV s^{-1}.

electroneutrality within the PEDOT film is mainly dominated by Li^+ insertion or extraction during the redox process. On the other hand, the role of ClO_4^- flux becomes more important when the DMSO or EG were used as the solvent. This indicates that the linear structure reveals more porous and promotes the migration of ions even with large anions such as ClO_4^-. Therefore, the PEDOT can rely on not only Li^+ but also ClO_4^- to satisfy the electroneutrality in 0.1 M $LiClO_4$–DMSO, which can enhance the reversibility of ionic transport.

In order to quantify the accumulated mass of PEDOT, the following redox reactions describing *p*-type doping and de-doping processes are proposed:

$$(PEDOT^+)(A^-) + x_R C^+ + (x_R - 1)A^- + e^- \rightarrow PEDOT[x_R AC] \quad (6)$$

$$PEDOT[x_R AC] + x_O C^+ + (x_O+1)A^- - e^- \rightarrow (PEDOT^+)(A^-)[(x_R + x_O)AC] \quad (7)$$

where A^- refers to ClO_4^-, and C^+ is either Li^+ or TBA^+. x_R and x_O represent stoichiometric number of cations for the reduction and oxidation processes, respectively, which can be determined by the following equations along with EQCM data. Positive and negative stoichiometric numbers respectively refer to insertion and extraction:

$$x_R = \frac{n_C|_{O\rightarrow R}}{\left|\frac{\Delta Q|_{O\rightarrow R}}{F}\right|} = \frac{n_C|_{O\rightarrow R}}{|(n_C\text{-}n_A)|_{O\rightarrow R}|} \quad (8)$$

$$x_O = \frac{n_C|_{R\rightarrow O}}{\left|\frac{\Delta Q|_{R\rightarrow O}}{F}\right|} = \frac{n_C|_{R\rightarrow O}}{|(n_C\text{-}n_A)|_{R\rightarrow O}|} \quad (9)$$

where $n_C|_{o\rightarrow R}$ and $n_C|_{R\rightarrow o}$ represent the amounts of cations exchanged within a PEDOT thin film in the reduction and oxidation processes, respectively. Similarly, $\Delta Q|_{R\rightarrow o}$ and $\Delta Q|_{o\rightarrow R}$ represent the accumulated charges passing through a PEDOT thin film during the reduction and oxidation processes, respectively.

With the known values of x_R and x_O (The detail results of x_R and x_O are shown in the supporting information), the redox reaction of a PEDOT which was cycled in 0.1 M $LiClO_4$–ACN solution between 0.3 and −0.9 V at the first cycle can be described by:

$$(PEDOT^+)(ClO^-_4) + 0.73Li^+ - 0.27ClO^-_4 + e^- \rightarrow PEDOT[0.73LiClO_4] \quad (10)$$

$$(PEDOT)(0.73LiClO_4) - 0.3Li^+ + 0.7ClO^-_4 - e^- \rightarrow (PEDOT^+)(ClO^-_4)[0.43LiClO_4] \quad (11)$$

From the redox equation, it can be seen that the amounts of Li^+ insertion and ClO_4^- extraction during the reduction process are not equal to that of Li^+ extraction and ClO_4^- insertion on the oxidation process, respectively. That means the behaviour of ionic transport within a PEDOT thin film is not reversible. Table 2 lists the amount of accumulated ion pairs for each electron involved when PEDOT was swept between 0.3 and −0.9 V in various solutions as a function of cycling number. The results reveal that ion pairs would accumulate in PEDOT thin films after each redox cycling. This is the main reason for the poor long-term stability of the polymer based devices such as Electrochromic or capacitor.[32] However, the amount of accumulated ion pairs is less when PEDOT is cycled in the $LiClO_4$–DMSO or EG solutions, as compared to that in the $LiClO_4$–ACN solution. This indicates the PEDOT under DMSO or EG can offer a highly ionic reversibility due to the conformational change from aggregated (ACN) to linear structure (DMSO and EG). These results are also consistent with the cycling stability in terms of charge capacity and molar flux mentioned above.

The redox behaviour of PEDOT films were further studied by *in situ* UV-vis absorption spectroscopy as indicated in Fig. 4. In the neutral state at −0.9 V, PEDOT has a maximum absorption due to the π–π* transition at about 600 nm. The features of the spectra are very similar from 0.3 to −0.5 V for the PEDOT in ACN and DMSO electrolytes as shown in Fig. 4 (a) and (b), respectively. The spectra show a little difference only below −0.5 V. The absorption of PEDOT in ACN electrolyte exhibits a shoulder at 900 nm even at −1.1 V. However, the absorption of PEDOT at 900 nm in DMSO electrolyte nearly vanishes just at −0.9 V, this means the PEDOT can not be completely reduced in ACN electrolyte. Such a completely reduced form of PEDOT in DMSO electrolyte offers a larger optical density change (ΔOD) of 0.6 at 600 nm, which is larger than 0.4 observed in ACN electrolyte. The largerΔOD is important for the electrochromic application which can offer a larger contrast. The difference in absorption of PEDOT for the two electrolytes can be due to the DMSO effect on the conformation of PEDOT chains. It is difficult for ion pairs to transport between PEDOT chains with aggregated conformation which impedes the redox reaction leading to an incompletely reduced form. After the aggregated structure transforms to the linear structure by the DMSO treatment, the PEDOT chains can attain completely reduced state.

To gain further information for the conductivity enhancement, the morphology was studied by AFM for the PEDOT treated with ACN and DMSO and are shown in Fig. 5. The morphology of PEDOT treated with ACN reveals a nano spherical aggregation assigned to the aggregated structure. However in the case of

Table 2 A summary of the amount of accumulated ion pair per e^- when PEDOT films were cycled in various electrolytes

	The amount of accumulated ion pair per e^-, $x_R + x_O$ ($LiClO_4$)							
Electrolyte (0.1 M $LiClO_4$)	1st cycle	2nd cycle	3rd cycle	4th cycle	5th cycle	10th cycle	50th cycle	100th cycle
ACN	0.432	0.350	0.310	0.300	0.289	0.250	0.174	0.151
DMF	0.398	0.245	0.163	0.119	0.104	0.087	0.045	0.015
EG	0.317	0.132	0.074	0.053	0.038	0.0151	0.004	0.003
DMSO	0.316	0.131	0.073	0.023	0.011	0.009	0.005	0.002

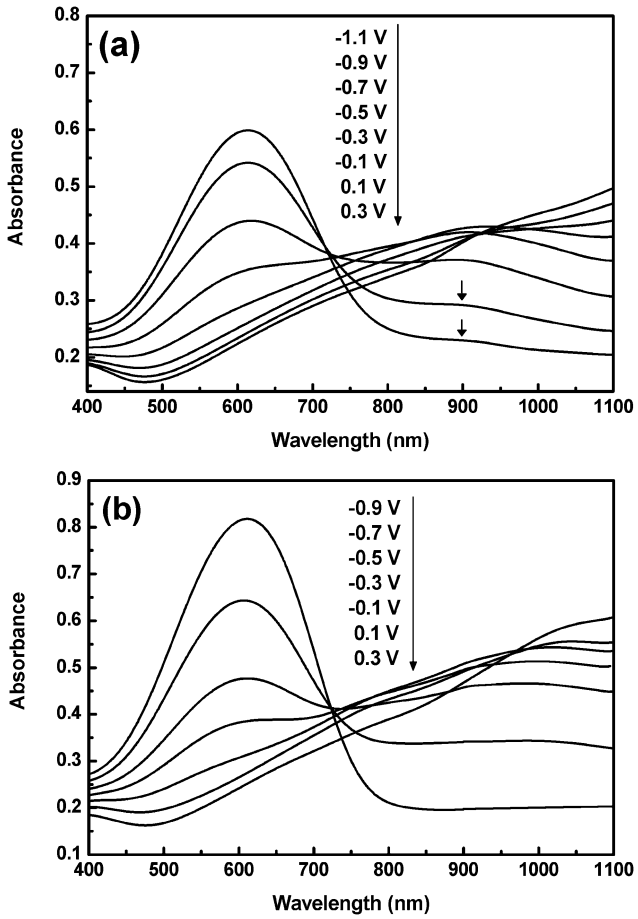

Fig. 4 *In situ* UV-vis absorption of PEDOT films at various potentials in (a) 0.1 M $LiClO_4$–ACN, (b) 0.1 M $LiClO_4$–DMSO.

the films treated with DMSO, the morphology shows a slightly flatter morphology compared with those treated with ACN. This change is due to the conformational change and the resultant increase in inter-chain interaction. These results support the PEDOT chains do undergo a transition from compact to extended-aggregated or linear in DMSO or EG, thereby enhancing both the hopping rate in the polymer and the ionic transport process in the polymer matrix.

Combining all the above mentioned results, we propose a model in Fig. 6 to explain the above results. When PEDOT is synthesized *via* oxidative polymerization, the polymer chain can not extend freely leading to a aggregated structure (Fig. 6 (a)). After treating with DMF or EG by cycling CV from 0.3 to −0.9 V, the interaction between the PEDOT chains and solvent and the driving force from the migration of ion pairs lead to a transition of polymer chains from aggregated to expanded-aggregated structure (Fig. 6 (b)). However, when the PEDOT treated with DMSO, the interaction become more significant and the PEDOT chains can be extend further to linear conformation (Fig. 6(d)). In this way, we can enhance the conductivity of PEDOT and promote the reversibility of ionic transport in the electrochemical system.

3.2 The performance of photovoltaic device with highly conductive PEDOT

Solar cells as a promising source of renewable and truly clean energy have become more and more attractive. Recently, focus on development of low band gap materials,[33–36] operational stability of devices[37–41] and processing in large areas[42,43] to achieve the industrial application have been extensively studied. Some efforts have been proposed to enhance the power conversion efficiency (PCE) *via* spectral coverage by incorporating low band gap materials to harvest the solar spectrum more efficiently. Other efficient ways to improve PCE is by means of modulating the energy level between electron donor and acceptor to increase open-circuit voltage (V_{OC}), using polyfluorene based co-polymer[44,45] and fullerene derivatives.[46] In this study, we fabricated the solar cell devices with the highly conductive PEDOT to reduce the series resistance (*R*s) leading to a higher fill factor (FF). Fig. 7 shows the *J*–*V* characteristics of the solar cell devices with PEDOT film treated from various solvents under 100 mW cm^{-2} AM1.5G illumination. The *J*–*V* curve of device with bare ITO as anode shows a obvious kink leading to a poor FF compared to those modified with PEDOT. These changes are explained by the higher work function of the PEDOT (5.2 eV) in

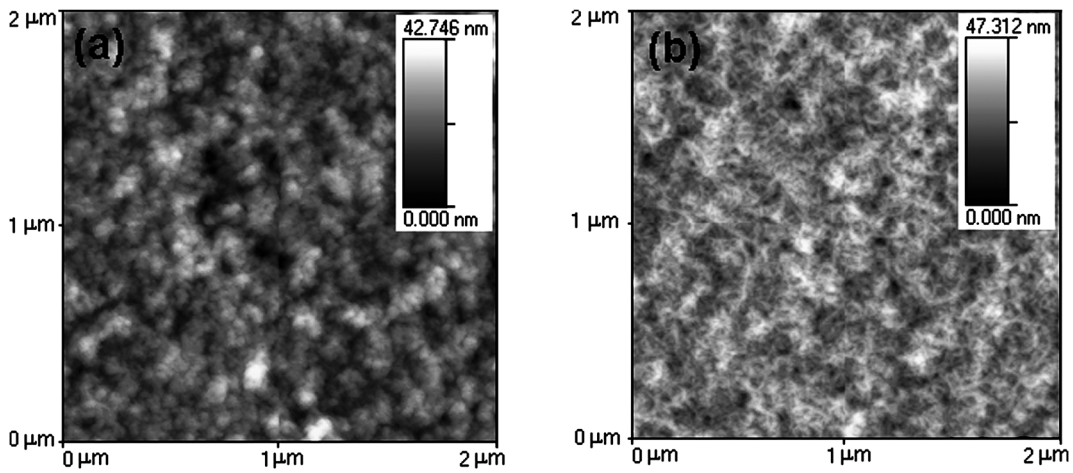

Fig. 5 The AFM images of (a) the pristine PEDOT (b) PEDOT treated with DMSO.

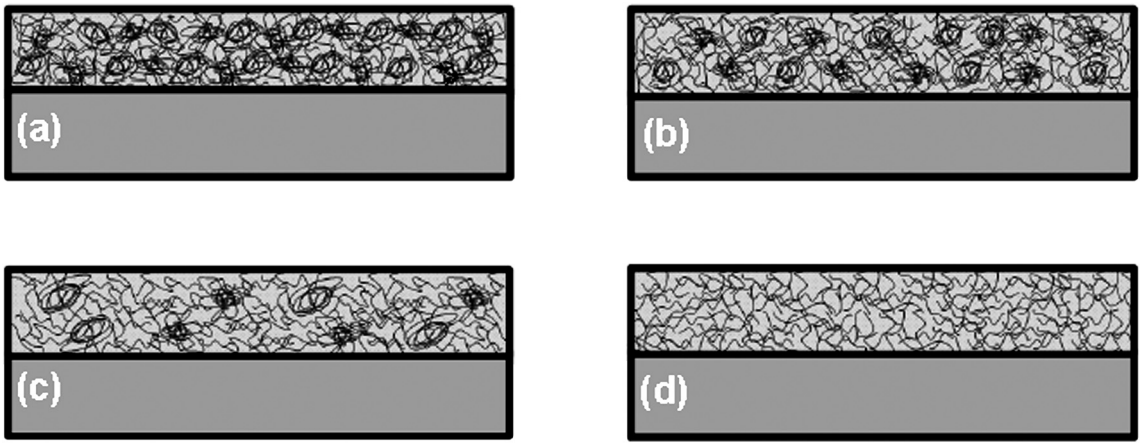

Fig. 6 Illustration of the differences in the polymer chain conformation. Blue wire: PEDOT polymer chain. (a) PEDOT without treatment, (b) treated with DMF, (c) treated with EG, (d) treated with DMSO.

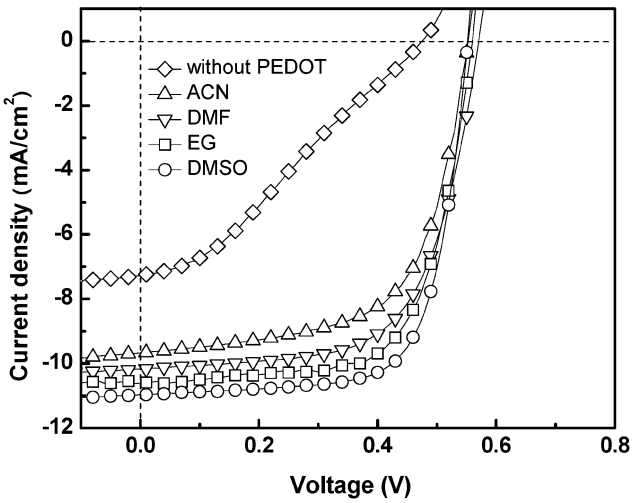

Fig. 7 *J–V* characteristics under illumination for photovoltaic devices based on P3HT–PCBM (1 : 0.8) with PEDOT layers treated from various solvents.

comparison with that of ITO (4.8 eV), which aligns well with the highest occupied molecular orbital (HOMO) of P3HT (5.2 eV) leading to a better hole injection. Therefore, the device without PEDOT results in a slow charge transfer at the interface between ITO electrode and the active layer. Consequently, the cell without PEDOT follows a *J–V* curves with inflection point due to the extremely imbalanced charge transport. The similar results have been reported in literature.[38,47–51] The device without PEDOT as buffer layer shows poor performance with V_{OC} = 0.47 V, J_{SC} = 7.27 mA cm^{-2} and FF = 26.8%. The calculated PCE is equal to 1.03%. On the other hand, the devices with PEDOT layer the V_{OC}, J_{SC} and FF all increase resulting in higher PCE. Furthermore, the device with PEDOT treated with DMSO reveals the largest FF compared with the one treated from other solvents, implying a lower *R*s. After treating with DMSO solvent, the FF can be improved to nearly 70%, indicating the PEDOT with higher conductivity reduces the series resistance of the photovoltaic devices. The similar results have also been reported previously.[52–56] Consequently, the device efficiency can be improved to 4.30%.

To further understand how the PEDOT treated with different solvents influences the resistance, the devices with different lateral distances between the anodes and cathodes have been fabricated and the corresponding *R*s is shown Fig. 8. It can been seen that the PEDOT treated with DMSO or EG reveal a lower *R*s compared with the one in ACN or DMF case, which is in agreement with the conductivities as shown in Table 1. Furthermore, Fig. 8 also shows an increase in *R*s with larger lateral distances, indicating the sheet resistance of ITO or PEDOT contribute to the device resistance. However, it is worthy to mention the slopes of the four devices with different PEDOT layers are almost the same, suggesting the sheet resistance is only contributed from the ITO electrode. The hole carrier can only be transported through the ITO layer in the lateral direction due to the much higher conductivity of ITO

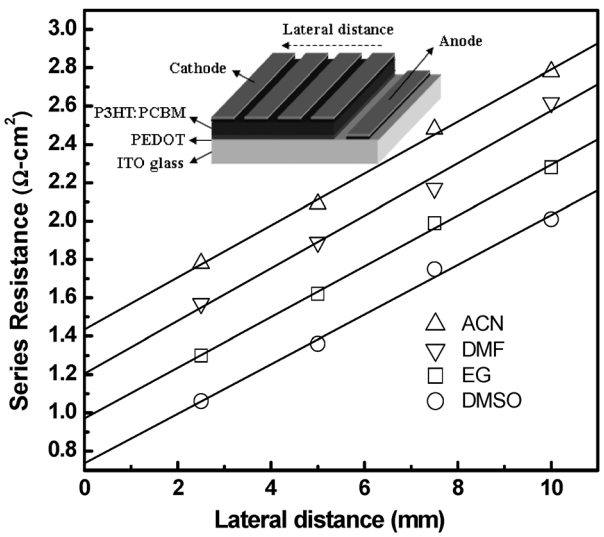

Fig. 8 Series resistance *R*s of the solar cells as function of the lateral distance between the anode and cathode with PEDOT layers treated from various solvents.

compared with that of PEDOT film. Even though, the conductivity of PEDOT has been enhanced significantly *via* treating with DMSO. The highly conductive PEDOT treated with DMSO promotes the series resistance significantly only in the vertical direction. The net series resistance of PEDOT can be calculated from the extrapolations of the fitting curves while the lateral distance equals to zero. The calculated resistance is only contributed from the PEDOT layer excluding the resistance between the cathode and anode in the lateral distance. The calculated resistance is 1.435, 1.205, 0.970 and 0.735 Ω cm^2 for the PEDOT treated with ACN, DMF, EG and DMSO solvent.

Recently, Kim *et. al.* have shown that the PEDOT with high conductivity can serve as an effective anode and generate excess photocurrent.[57] To investigate this issue, we measured the devices with different illuminated area as shown in Fig. 9. Table 3 shows the solar cells based on PEDOT treated with DMSO with different exposed area. Although the highly conductive PEDOT can also serve as an anode and increase the photo-generated holes, the photocurrent of the solar cells with different exposed area is almost the same in our cases which is quite differ from the previous work.[53] The invariable photocurrent based on the experimental results is due to the extremely balanced charge transport. In order to validate the presumption, we fabricated electron and hole only devices. The *J*–*V* curves of electron and hole only devices are shown in Fig. 10. Here, we correct voltage (V_{appl}) with built-in potential (V_{bi}) using $V = V_{appl} - V_{bi}$. The curves were fitted with space-charge limited current (SCLC) model to calculate charge mobility. he calculation used $J = 9\varepsilon_0\varepsilon_r\mu V^2/8L^3$,[58] where $\varepsilon_0\varepsilon_r$ is the permittivity of the polymer, μ is the carrier mobility and L is the device thickness. The electron (μ_e) and hole mobility (μ_h) calculated from the SCLC model are 2.20×10^{-7} and 1.84×10^{-7} m^2 Vs, respectively.

It can be found the solar cell devices with extremely balanced charge mobility ($\mu_e/\mu_h = 1.20$). This means that although the PEDOT with high conductivity can transport photo-generated holes as an additional anode, the photocurrent is still limited by the transport rate of electrons. Furthermore, it can also be seen that the charge transport in the lateral distance is dominated by the ITO glass as evident from the identical slope from Fig. 8. Therefore, the highly conductive PEDOT can not acts as an additional anode based on these reasons but will help in effective hole transport. Hence the photocurrent is independent of the illumination area in our case.

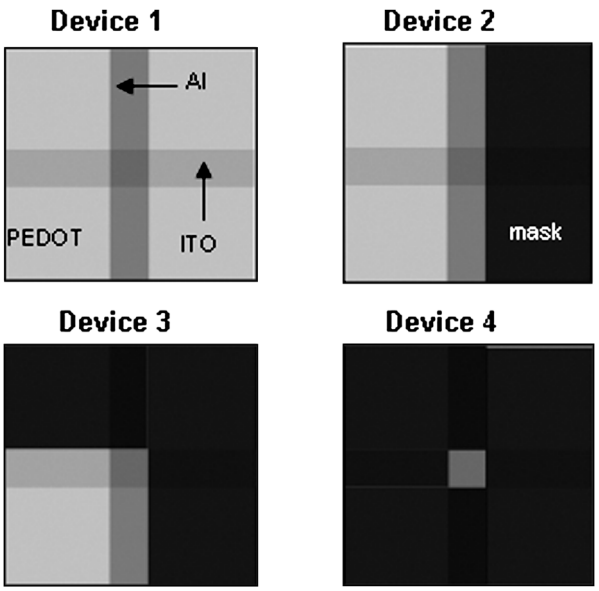

Fig. 9 Scheme of solar cells under different masks to control the illumination area.

Table 3 A summary of the cell performance of parameters, indicating J_{SC}, V_{OC}, FF and PCE as a function of illumination area

Sample[a]	J_{SC}/mA cm^{-2})	V_{OC}/V	FF (%)	PCE (%)
Device 1	10.96	0.56	70.0	4.30
Device 2	10.50	0.56	70.3	4.13
Device 3	11.04	0.56	69.5	4.29
Device 4	10.28	0.56	70.4	4.05

[a] All the devices were fabricated with PEDOT treated from DMSO solvent.

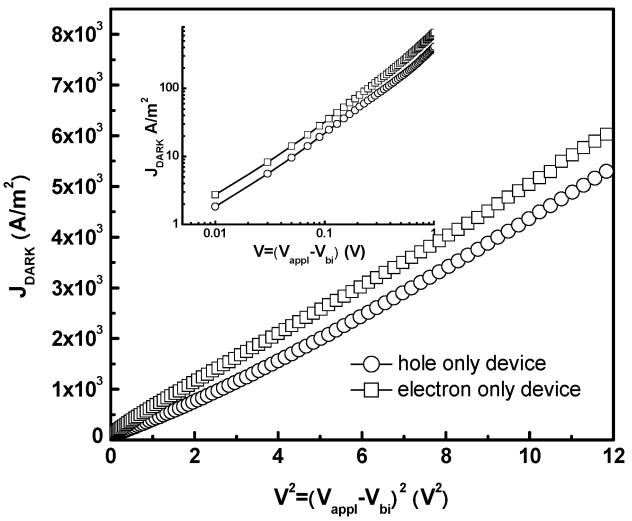

Fig. 10 *J*–*V* curves for electron and hole only devices based on P3HT–PCBM with PEDOT treated from DMSO.

4. Conclusion

In the present study, the conductivity of PEDOT was enhanced by treating it with DMSO or EG solvents. The conductivity enhancement of PEDOT is contributed from the interaction between the dipole of the organic solvents and the dipoles or charges on the PEDOT chains. With the existence of DMSO and EG, the polymer chains can be changed from aggregated to linear structure. This offers a higher conductivity, better cycling stability and reversibility of ionic transport during redox process. We employed the highly conductive PEDOT as a replacement for commercial PEDOT–PSS to construct the photovoltaic devices. The PEDOT treated with DMSO can enhance the FF of photovoltaic device due to its high conductivity. Therefore an

entirely positive effect in terms of solar cell efficiency has also been observed in this study.

Acknowledgements

The authors are also grateful to the National Science Council (NSC), Taiwan, (NSC 97-2120-M-002-012 and NSC 96-2221-E-001-017-MY2) and Thematic Research Program of Academia Sinica, Taiwan for financial support.

References

1 C. J. Ko, Y. K. Lin, F. C. Chen and C. W. Chu, *Appl. Phys. Lett.*, 2007, **90**, 063509.
2 F. L. Zhang, A. Gadisa and O. Inganäs, *Appl. Phys. Lett.*, 2004, **84**, 3906.
3 S. Ghosh and O. Inganäs, *Synth. Methods*, 2001, **121**, 1321.
4 L. A. A. Pettersson, S. Ghosh and O. Inganäs, *Org. Electron.*, 2002, **3**, 143.
5 S. Ashizawa, R. Horikawa and H. Okuzaki, *Synth. Methods*, 2005, **153**, 5.
6 S. Timpanaro, M. Kemerink, F. J. Touwslager, M. M. De Koc and S. Schrader, *Chem. Phys. Lett.*, 2004, **394**, 339.
7 H. J. Snaith, H. Kenrick, M. Chiesa and R. H. Friend, *Polymer*, 2005, **46**, 2573.
8 J. Y. Kim, J. H. Jung, D. E. Lee and J. Joo, *Synth. Methods*, 2002, **126**, 311.
9 S. K. M. Jönsson, J. Birgerson, X. Crispin, G. Greezynski, W. Osikowicz, A. W. D. van der Gon, W. R. Salaneck and M. Fahlman, *Synth. Methods*, 2003, **139**, 1.
10 X. Crispin, S. Marciniak, W. Osikowicz, G. Zotti, A. W. Denier van der Gon, F. Louwet, M. Fahlman, L. Groenendaal, F. de Schryver and W. R. Salaneck, *J. Polym. Sci. Polym. Phys.*, 2003, **41**, 2561.
11 J. Ouyang, Q. Xu, C. W. Chu, Y. Yang, G. Li and J. Shinar, *Polymer*, 2004, **45**, 8443.
12 D. Bagchi and R. Menon, *Chem. Phys. Lett.*, 2006, **425**, 114.
13 Y. H. Ha, N. Nikolov, S. K. Pollack, J. Mastrangelo, B. D. Martin and R. Shashidhar, *Adv. Funct. Mater.*, 2004, **14**, 615.
14 T. Y. Kim, J. E. Kim and K. S. Suh, *Polym. Int.*, 2006, **55**, 80.
15 G. Sauerbery, *Z. Phys.*, 1959, **155**, 206.
16 V. Shrotriya, G. Li, Y. Yao, C. W. Chu and Y. Yang, *Appl. Phys. Lett.*, 2006, **88**, 073508.
17 V. Shrotriya, Y. Yao, G. Li and Y. Yang, *Appl. Phys. Lett.*, 2006, **89**, 063505.
18 W. Plieth, A. Bund, U. Rammelt, S. Neudeck and L. Duc, *Electrochim. Acta*, 2006, **51**, 2366.
19 A. Aleshin, R. Kiebooms, R. Menon and A. J. Heeger, *Synth. Methods*, 1997, **90**, 61.
20 M. Strange, D. Plackett, M. Kaasgaard and F. C. Krebs, *Sol. Energy Mater. Sol. Cells.*, 2008, **92**, 805.
21 K. Tvingstedt and O. Inganäs, *Adv. Mater.*, 2007, **19**, 2893.
22 A. Gadisa, K. Tvingstedt, S. Admassie, L. Lindell, X. Crispin, M. R. Andersson, W. R. Salaneck and O. Inganäs, *Syth. Methods*, 2006, **156**, 1102.
23 B. W. Jensen and F. C. Krebs, *Sol. Energy Mater. Sol. Cells.*, 2006, **90**, 123.
24 T. Aernouts, P. Vanlaeke, W. Geens, J. Poortmans, P. Heremans, S. Borghs, R. Mertens, R. Andriessen and L. Leenders, *Thin Solid Films*, 2004, **451**, 22.
25 J. Y. Lee, S. T. Connor, Y. Cui and P. Peumans, *Nano Lett.*, 2008, **8**, 689.
26 C. Weidlich, K. M. Mangold and K. Jüttner, *Electrochim. Acta*, 2005, **50**, 1547.
27 L. P. Bauermann and P. N. Bartlett, *Electrochim. Acta*, 2005, **50**, 1537.
28 S. L. de Albuquerque Maranhao and R. M. Torresi, *J. Electrochem. Soc.*, 1999, **146**, 4179.
29 G. Maia, R. M. Torresi, E. A. Ticianelli and F. C. Nart, *J. Phys. Chem.*, 1996, **100**, 15910.
30 S. L. de Albuquerque Maranhao and R. M. Torresi, *J. Electrochem. Soc.*, 1999, **146**, 4179.
31 M. Ue, *J. Electrochem. Soc.*, 1994, **141**, 3336.
32 C. W. Chang and G. S. Liou, *Org. Electron.*, 2007, **8**, 662.
33 S. Günes, H. Neugebauer and N. S. Sariciftci, *Chem. Rev.*, 2007, **107**, 1324.
34 J. Bouclé, P. Ravirajan and J. Nelson, *J. Mater. Chem.*, 2007, **17**, 3141.
35 E. Bundgaard and F. C. Krebs, *Sol. Energy Mater. Sol. Cells.*, 2007, **91**, 954.
36 B. C. Tompson and J. M. J. Fréchet, *Angew. Chem., Int. Ed.*, 2008, **47**, 58.
37 M. Jørgensen, K. Norrman and F. C. Krebs, *Sol. Energy Mater. Sol. Cells.*, 2008, **92**, 686.
38 F. C. Krebs and K. Norrman, *Prog. Photovolt. Res. Appl.*, 2007, **15**, 697.
39 G. Li and Y. Yang, *Nanotechnology*, 2008, **19**, 424014.
40 F. C. Krebs, *Sol. Energy Mater. Sol. Cells.*, 2008, **92**, 715.
41 C. Y. Li, T. C. Wen, T. H. Lee, T. F. Guo, J. C. A. Huang, Y. C. Lin and Y. J. Hsu, *J. Mater. Chem.*, 2009, **19**, 1643.
42 E. Bundgaard and F. C. Krebs, *Sol. Energy Mater. Sol. Cells.*, 2007, **91**, 1019.
43 M. Niggemann, B. Zimmermann, J. Haschke, M. Glatthaar and A. Gombert, *Thin Solid Films*, 2008, **516**, 7181.
44 J. H. Huang, Z. Y. Ho, D. Kekuda, Y. Chang, C. W. Chu and K. C. Ho, *Nanotechnology*, 2009, **20**, 025202.
45 J. H. Huang, C. Y. Yang, Z. Y. Ho, D. Kekuda, M. C. Wu, F. C. Chien, P. Chen, C. W. Chu and K. C. Ho, *Org. Electron.*, 2009, **10**, 27.
46 M. Lenes, G. A. H. Wetzelaer, F. B. Kooistra, S. C. Veenstra, J. C. Hummelen and P. W. M. Blom, *Adv. Mater.*, 2008, **20**, 2116.
47 M. Vogel, S. Doka, C. Breyer, M. C. L. Steiner and K. Fostiropoulos, *Appl. Phys. Lett.*, 2006, **89**, 163501.
48 S. T. Zhang, Y. C. Zhou, J. M. Zhao, Z. J. Wang, Y. Wu, X. M. Ding and X. Y. Hou, *Appl. Phys. Lett.*, 2006, **89**, 043502.
49 M. Glatthaar, M. Riede, N. Keegan, K. S. Hvid, B. Zimmermann, M. Niggemann, A. Hinsch and A. Gombert, *Sol. Energy Mater. Sol. Cells.*, 2007, **91**, 390.
50 P. Peumans and S. R. Forrest, *Appl. Phys. Lett.*, 2001, **79**, 126.
51 F. Zhang, M. Johansson, M. R. Andersson, J. C. Hummelen and O. Inganäs, *Adv. Mater.*, 2002, **14**, 662.
52 J. Ouyang, C. W. Chu, F. C. Chen, Q. Xu and Y. Yang, *Adv. Funct. Mater.*, 2006, **15**, 203.
53 E. Ahlswede, W. Mühleisen, M. W. bin Moh Wahi, J. Hanisch and M. Powalla, *Appl. Phys. Lett.*, 2008, **92**, 143307.
54 Y. S. Hsiao, W. T. Whang, C. P. Chen and Y. C. Chen, *J. Mater. Chem.*, 2008, **18**, 5848.
55 J. H. Huang, Z. Y. Ho, D. Kekuda, C. W. Chu and K. C. Ho, *J. Phys. Chem. C*, 2008, **112**, 19125.
56 C. Y. Li, T. C. Wen and T. F. Guo, *J. Mater. Chem.*, 2008, **18**, 4478.
57 M. S. Kim, M. G. Kang, L. J. Guo and J. Kim, *Appl. Phys. Lett.*, 2008, **92**, 133301.
58 W. D. Gill, *J. Appl. Phys.*, 1972, **43**, 5033.

